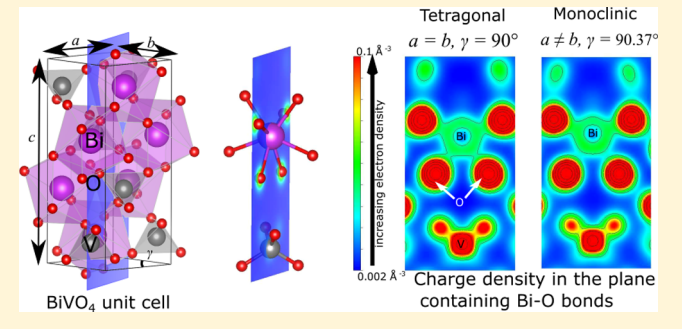
# Effects of Doping on the Crystal Structure of BiVO<sub>4</sub>

Iflah Laraib, † Marciano Alves Carneiro, †,‡ and Anderson Janotti\*,†

**ABSTRACT:** The search for efficient photoelectrochemically active materials has led to several studies on BiVO<sub>4</sub>, which has shown higher photocurrent than most typical semiconductors under photoelectrochemical (PEC) operation. BiVO<sub>4</sub> can be stabilized in different crystal structures, yet high PEC efficiency is found only for n-type doped monoclinic phase. The theoretical description of the monoclinic polymorph is difficult because of spontaneous transformation to a tetragonal phase. The cause of such instability of the monoclinic phase has yet to be resolved. Using first-principles calculations based on density functional theory, we explore how the concentration of excess electrons in this material affects its phase



stability. We analyze the unit-cell structure, local bonding, and band structure of BiVO<sub>4</sub> at different concentrations of excess electrons. We find that as the concentration of excess electrons increases, the tetragonal phase spontaneously transforms into the monoclinic phase, suggesting a crucial role of doping in the structure and, thus, the photoelectrochemical performance of BiVO<sub>4</sub>.

## ■ INTRODUCTION

Heightened environmental awareness in recent decades has fueled research on renewable sources to meet the growing demand for energy. Hydrogen generation has been considered one of the possible solutions for a low-carbon economy. 1,2 Researchers have proposed that a sustainable hydrogen producing apparatus in the form of a photoelectrochemical (PEC) cell can be setup by tapping sunlight to perform photolysis or water splitting via artificial photosynthesis. This process was first reported in 1972 by Fujishima and Honda, who used UV illuminated TiO2 electrodes to perform electrochemical photolysis of water.<sup>3</sup> PEC cells have since emerged as monoliths for harvesting sunlight to directly obtain H<sub>2</sub> gas.<sup>4-6</sup> It has been concluded through extensive studies that material properties such as visible light absorption, <sup>7</sup> charge carrier separation,<sup>8</sup> and stability under operation<sup>9</sup> are crucial for efficient solar-to-hydrogen conversion during PEC process. Although several semiconducting materials are available for use as photoelectrodes, BiVO<sub>4</sub>, in particular, has demonstrated promising behavior as a PEC anode. 7,9 The high performance of this material has been attributed to the almost ideal position of the conduction-band minimum and valence-band maximum with respect to the water oxidation/reduction levels, leading to enhanced photoabsorption and consequential  $H_2$  evolution. The presence of donor defects such as interstitial hydrogen or oxygen vacancies was reported to be crucial for the enhanced PEC performance of the monoclinic phase of BiVO<sub>4</sub>, <sup>12-14</sup> the cause of which is yet under debate.

BiVO<sub>4</sub> is known to exist in four different phases or polymorphs, namely, orthorhombic, zircon-tetragonal, monoclinic (m), and tetragonal (t). 15,16 Although the orthorhombic phase is the most common phase in which BiVO<sub>4</sub> occurs in nature, generally known as the mineral pucherite, it has not been synthesized in the laboratory. 17 Low-temperature synthesis of BiVO<sub>4</sub> yields the zircon-tetragonal phase, which has a band gap of 2.9 eV. 18 Upon heating the zircon phase to 528 K, 17,19 BiVO<sub>4</sub> transforms into the m phase, which can be reversibly converted to t-BiVO<sub>4</sub> by tuning of temperature. In these crystal structures, V is coordinated by four O atoms in a tetrahedral site and each Bi is coordinated by eight O atoms from eight different VO<sub>4</sub> tetrahedral units. The only difference between t-BiVO<sub>4</sub> and m-BiVO<sub>4</sub> is that the VO<sub>4</sub> and BiO<sub>8</sub> polyhedra in t-BiVO<sub>4</sub> are symmetric, while those in m-BiVO<sub>4</sub> are not. 20-23 The reported band gaps of both t-BiVO<sub>4</sub> and m-BiVO<sub>4</sub> are indirect and lie between 2.3 and 2.4 eV. <sup>10,18</sup>

In experimental studies, the unit cells of t-BiVO<sub>4</sub> and m-BiVO<sub>4</sub> are often reported in I-centered (body centered) I4<sub>1</sub>/a and I2/b space groups, respectively, as are shown in Figure 1a,b. In most computational studies, however, a standard representation of m-BiVO<sub>4</sub> in the C2/c space group has been used [Figure 1c,d]. 11,24,25 The advantage of using the unit cell of m-BiVO<sub>4</sub> in the I2/b space group is that it can be easily compared to the structure of t-BiVO<sub>4</sub>, except that in the former, the lattice parameter a slightly differs from b and the angle  $\gamma$  is only slightly over 90°, so that it is easy to distinguish the two phases. <sup>13</sup> The standard monoclinic C-centered C2/crepresentation of m-BiVO<sub>4</sub> in Figure 1c can be carved out of the I2/b one, as shown by the shaded region in Figure 1d.

Received: June 19, 2019 Revised: September 18, 2019 Published: October 9, 2019

Department of Materials Science and Engineering, University of Delaware, Newark, Delaware 19716, United States

<sup>&</sup>lt;sup>‡</sup>Universidade Federal Fluminense, Niterói, Rio de Janeiro 24210-346, Brazil

The Journal of Physical Chemistry C

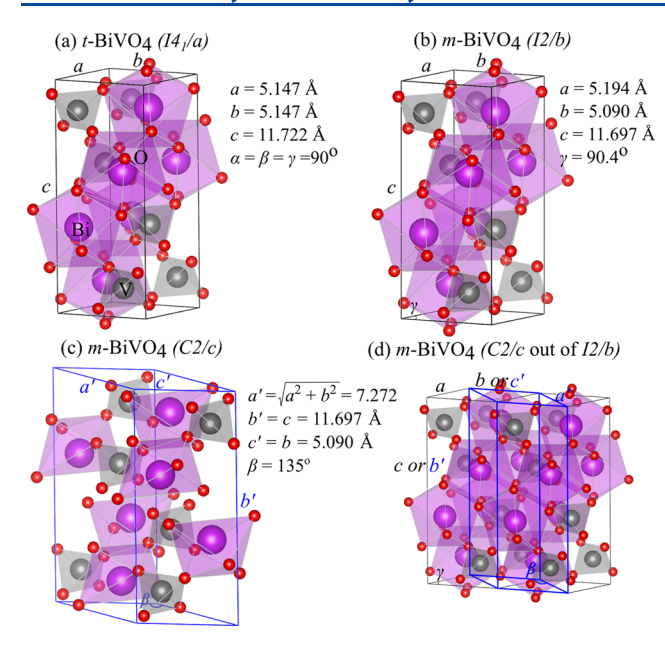


Figure 1. Polyhedral representation of conventional unit cells of (a) t-BiVO<sub>4</sub> and (b) m-BiVO<sub>4</sub>. The C2/c representation of m-BiVO<sub>4</sub> shown in (c) can be carved out from the I2/b m-BiVO<sub>4</sub>, as shown in (d).

Despite extensive research on PEC performance of m-BiVO<sub>4</sub>, subtle yet significant discrepancies in the theoretical description of its crystal structure still exist. When optimizing the lattice parameters and atomic positions of m-BiVO<sub>4</sub>, using density functional theory (DFT) calculations within standard approximations for the exchange and correlation, it spontaneously transforms to the t phase, such that many of the reports on this material end up incorrectly using t-BiVO<sub>4</sub> instead of m-BiVO<sub>4</sub>. Since most recent computational studies use the C2/c unit cell, which is difficult to compare with t-BiVO<sub>4</sub> because it does not resemble the  $I4_1/a$  structure, this transformation has been largely overlooked. Kweon et al. stabilized the m phase (I2/b space group) by tuning the extent Hartree–Fock mixing (50%) in hybrid density functional calculation  $^{26}$ 

We note that m-BiVO<sub>4</sub> can be viewed as a layered structure, as seen in Figure 1b, compared to the tridimensional structure of t-BiVO<sub>4</sub> shown in Figure 1a. One then expects that adding electrons to bands derived from V-O antibonding states of t-BiVO<sub>4</sub> (i.e., the lowest-energy conduction bands, as discussed below) may lead to a lengthening of some of the V-O bonds, and, therefore, to a more asymmetric structure such as that of m-BiVO<sub>4</sub>. We, therefore, hypothesize that the stabilization of m-BiVO<sub>4</sub> can be enabled by the presence of excess electrons in the conduction band, which can be accomplished through doping. These excess electrons tend to elongate bonds, leading to lower crystal-structure symmetry. Indeed, the reported PEC activity of m-BiVO<sub>4</sub> invariably happens to involve an n-type doped material.<sup>27</sup> Motivated by this hypothesis, we use DFT calculations to study the effects of excess electrons on the phase stability of BiVO<sub>4</sub>. We find that t-BiVO<sub>4</sub> spontaneously transforms into m-BiVO<sub>4</sub>, as the carrier density increases. Without worrying about the specific nature of the shallow donor defects or impurities, in this work, we will present an analysis of the effects of adding excess electrons to the conduction band on the local bonding, crystal structure, and electronic structure of BiVO<sub>4</sub>.

#### COMPUTATIONAL DETAILS

The calculations are based on DFT, <sup>28,29</sup> as implemented in the Vienna Ab initio Simulation (VASP) code. 30,31 The projector augmented wave (PAW) method is used to describe the interaction between the core and valence electrons.<sup>32</sup> For the exchange and correlation term, we test various functionals including the generalized gradient approximation (GGA) of Perdew-Burke-Enzerhof (PBE), 33 PBE revised for solids (PBEsol),<sup>34</sup> the metageneralized gradient approximation based on the Strongly Constrained and Appropriately Normed (meta-GGA SCAN) formalism,<sup>35</sup> and the screened hybrid functional of Heyd, Scuseria, and Enzerhof (HSE06).<sup>36</sup> Selfconsistent total-energy calculations are performed on conventional unit cells consisting of 24 atoms to optimize the structures of m- and t-BiVO<sub>4</sub>. All calculations are performed using a plane-wave basis set with a cutoff of 520 eV and a 12 ×  $12 \times 6$  Γ-centered k-point mesh for integrations over the Brillouin zone.

Doping is simulated by the addition of excess electrons to the unit cell; we added up to 0.25 electrons per formula unit, in steps of 0.03125 electrons, which corresponds to adding up to 1 electron per unit cell, in steps of 0.125 electron. This corresponds to adding up to  $3.14 \times 10^{21}$  electrons/cm³. A neutralizing homogeneous background is added to ensure convergence. All lattice parameters and atomic positions are allowed to relax until the atomic forces reach a maximum threshold of 0.01 eV/Å. Note that in this way, we avoid the influence of the chemical nature of the impurity and the results should, in principle, be valid for any shallow donor impurity or can represent an electrically charged region near the surface or interface due to band bending.

In the tests using the HSE functional, we were limited to  $2 \times 2 \times 1$  mesh of k-points, making the calculations less accurate, in particular, those involving a metallic state, i.e., with electrons in the conduction band. Overall, the results using different functionals lead essentially to the same conclusions, except that calculated equilibrium lattice parameters slightly differ for different functionals.

The nonself consistent calculations (band structure and density of states) are done on neutrally charged unit cells. The nature of band gaps remained the same for different functionals, but the values of band gaps for HSE06 functional were significantly higher than the experimental values. Thus, the band gap was not corrected by HSE06, and further investigation of the correct mixing and screening parameters for the band gap correction in BiVO<sub>4</sub> is underway. In the following, we present the results using meta-GGA SCAN.

# RESULTS

We begin by describing the experimentally reported conventional unit-cell structures of t-BiVO<sub>4</sub> belonging to the  $I4_1/a$  space group, m-BiVO<sub>4</sub> belonging to the I2/b space group<sup>21</sup> and C2/c space group, as shown in Figure 1a—c.

Although in t-BiVO<sub>4</sub>, we have four V–O bonds with equal length, in m-BiVO<sub>4</sub>, the V–O bond lengths are separated in two groups of two, differing by 0.08 Å. The eight Bi–O bond lengths are separated in two groups of four with difference of only 0.04 Å in t-BiVO<sub>4</sub>, while in m-BiVO<sub>4</sub>, the Bi–O form a much less symmetric polyhedral with bond lengths separated in four groups of two, with differences varying from 0.27, 0.16, and 0.02 Å from the longest to the shortest group, as indicated in Figure 2.

The Journal of Physical Chemistry C

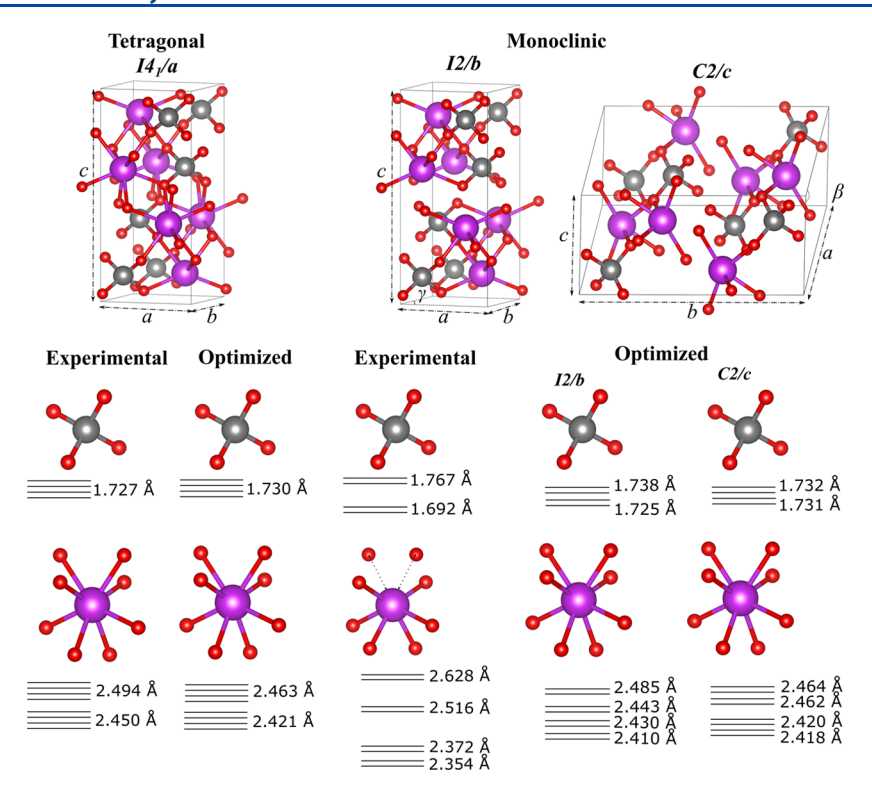


Figure 2. Unit cells and local structures of the two different phases, with corresponding Bi(V)—O bond lengths represented by horizontal lines (not drawn to scale), both as per experimental reports and after optimization of t-BiVO<sub>4</sub> and m-BiVO<sub>4</sub>. Groups of horizontal lines indicate a number of metal—oxygen bonds with equal length.

Starting from the experimental data for t-BiVO<sub>4</sub>, m-BiVO<sub>4</sub> in the I2/b unit cell, and m-BiVO<sub>4</sub> in the C2/c unit cell, we optimized the volume and atomic positions of the three unit cells and analyzed their structure. The results of the optimization are illustrated in Figure 2, and the lattice parameters (both before and after optimization) are also listed in Table 1. By inspecting the metal—oxygen bond lengths, we

Table 1. Lattice Parameters of t- and m-BiVO<sub>4</sub>, As Reported Experimentally,<sup>21</sup> and Obtained by Meta-GGA SCAN Calculations Without and With 0.250 Excess Electron Per Formula Unit

		meta-GGA SCAN	
phase	experiment	without extra electron	with extra electron
t-BiVO <sub>4</sub>	a = b = 5.147  Å	a = b = 5.110  Å	a = b = 5.113 (Å)
	c = 11.722  Å	c = 11.607  Å	c = 11.605  Å
	$\alpha=\beta=\gamma=90^\circ$	$\alpha=\beta=\gamma=90^\circ$	$\alpha=\beta=\gamma=90^\circ$
	a = 5.194  Å	a = 5.123  Å	a = 5.241  Å
m-BiVO <sub>4</sub>	b = 5.09  Å	b = 5.107  Å	b = 5.135  Å
	c = 11.697  Å	c = 11.594  Å	c = 11.833  Å
	$\gamma = 90.4^{\circ}$	$\gamma = 90^{\circ}$	$\gamma = 90.22^{\circ}$
	a/b = 1.02	a/b = 1.00	a/b = 1.02

observe that the unit cells of m-BiVO<sub>4</sub> (both I2/b and C2/c) spontaneously transform to t phase upon optimization. From the values of bond lengths reported in Figure 2, it is clear that the unit-cell structure of m-BiVO<sub>4</sub> becomes more symmetric compared to the experimental structure, while t-BiVO<sub>4</sub> retains its initial 4-fold symmetry after optimization. We also note that the lattice parameters of the I2/b unit cell  $(a, b, and \gamma)$  showed a significant shift from initial (experimental) values for m-

BiVO<sub>4</sub> toward those of t-BiVO<sub>4</sub>, while it would be difficult to see such transformation by only inspecting the optimized lattice parameters for the C2/c unit cell. It is also necessary to check the changes in its local structure, which are key to making a clear distinction between m and t phases. These results lead us to conclude that the C2/c unit cell is not ideal for studying the structure of m-BiVO<sub>4</sub>, because by inspecting only the optimized lattice parameters, it is difficult to distinguish m-BiVO<sub>4</sub> from t-BiVO<sub>4</sub>. In the rest of the paper, we, therefore, proceeded by studying m-BiVO<sub>4</sub> using the I2/b unit cell, and, henceforth, all mention of m-BiVO<sub>4</sub> shall refer solely to the I2/b m-BiVO<sub>4</sub>.

In the following, we study the changes in the crystal structure of m-BiVO<sub>4</sub> upon addition of excess electrons in its conduction band, fully optimizing lattice parameters and atomic positions.

Effects of Doping on the Local Structure. We investigate the evolution of the local structure of BiVO4 in the presence of excess electrons by measuring bond lengths in VO<sub>4</sub> and BiO<sub>8</sub> polyhedra and plotting them against the number of excess electrons. The plots shown in Figure 3 demonstrate an increasing disparity between bond lengths within the constituent polyhedra, as we move from 0 to 0.250 excess electron per formula unit. Thus, the presence of excess electrons in the unit cell causes nonuniform stretching and compressing of the metal-oxygen bonds, consequently leading to a lower symmetry in the polyhedra. The results in Figure 3 indicate that the local structure of  $BiVO_4$  shifts from t to m with increasing concentration of excess electrons. We can see that two of the Bi-O bonds are elongated by 7%, while two of the V-O bonds are elongated by 3% upon addition of 0.250 electrons per formula unit, turning the undoped tridimensional

The Journal of Physical Chemistry C

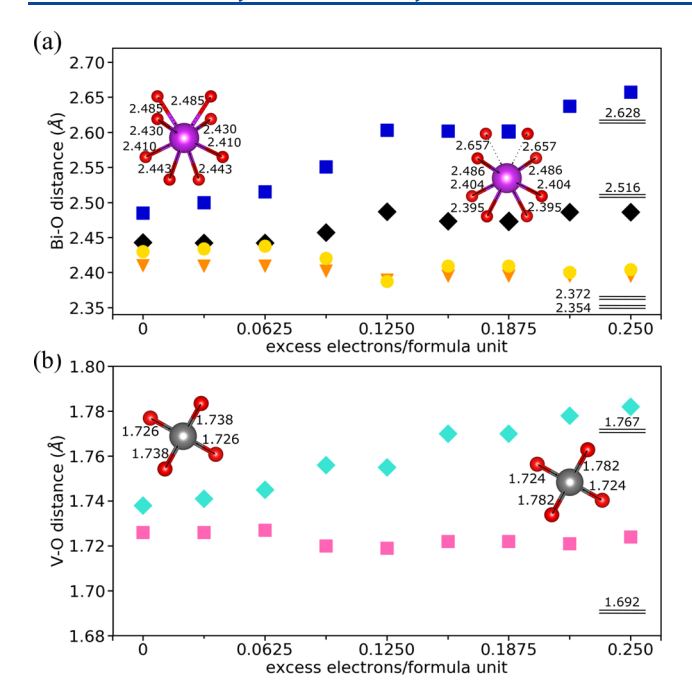
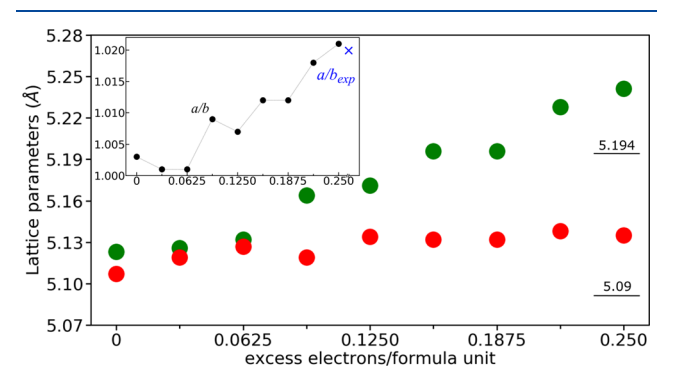


Figure 3. Bi-O (top) and V-O (bottom) bond distances in  $BiVO_4$  with respect to excess electron concentration. The numbers on the motifs on the left and right corners of the plots indicate the bond distances in Å for  $BiVO_4$  optimized without excess electrons and with 0.250 excess electrons per formula unit, respectively. The horizontal lines indicate pairs of Bi(V)-O bond lengths as per experimental reports. <sup>21</sup>

structure into a layered structure, as reported experimentally for m-BiVO $_4$ .

**Effects of Doping on Lattice Parameters.** To quantify the extent of the resemblance of the optimized unit cell with m- or t-phase BiVO<sub>4</sub>, we plot in Figure 4, the values of the



**Figure 4.** Lattice parameters a and b, along with their ratio a/b (shown in the inset) with respect to increasing concentration of excess free electrons in the BiVO<sub>4</sub> unit cell. The horizontal lines indicate lattice parameters (a and b) as per experimental reports. <sup>21</sup>

lattice parameters a and b and the ratio a/b with respect to the concentration of excess electrons. At the low concentration of excess electrons (between 0 and 0.0625 electrons per formula unit), symmetry of the unit cell of t-BiVO<sub>4</sub> remains intact (i.e., a=b, a/b=1), but after sufficient excess electrons are added (approximately 0.094 per formula unit), the structure spontaneously transforms to m-BiVO<sub>4</sub> ( $a \neq b, a/b > 1$ ). At 0.25 excess electron per formula unit, the ratio a/b is approximately equal to the experimental value, as shown in the inset of Figure 3. This is in line with our initial observation

from studying the changes in the local structure of BiVO<sub>4</sub>. Thus, we conclude that the concentration of excess electrons in BiVO<sub>4</sub> strongly affects its phase as the unit cell transforms from t to m symmetry.

Band Structures of t-BiVO<sub>4</sub> and m-BiVO<sub>4</sub>. It has been established that both m- and t-BiVO<sub>4</sub> have indirect band gaps between 2.3 and 2.4 eV. 11,19 Although PBE or PBEsol functionals underestimate the band gap of BiVO<sub>4</sub> by about 0.7 eV, our calculations using the hybrid functional HSE06, i.e., with standard mixing and screening parameters  $\alpha = 0.25$  and  $\mu$ =  $0.207 \text{ Å}^{-1}$ , overestimate the reported band gap by about 0.9 eV. Previous HSE calculations<sup>26</sup> show that the experimental band gap can be reproduced by reducing the mixing parameter to 0.05 (i.e., 5% of Hartree-Fock exchange mixed with 95% of PBE exchange). Their reported band gap using standard mixing and screening parameters amounts to 3.5 eV.<sup>26</sup> More recently, it was reported that the apparent agreement between semilocal functionals or hybrid functional with a small fraction of Hartree-Fock exchange is due to error cancellation,<sup>37</sup> and that the calculated absorption spectrum using HSE or the quasiparticle GW method is in good agreement with the experiment when excitonic effects, nuclear motion, and finite temperature vibrations are included.3

The calculated band structures of undoped m- and t-BiVO<sub>4</sub>, using the meta-GGA SCAN functional, are displayed in Figure 5a,b to show the similarities between the two phases regarding

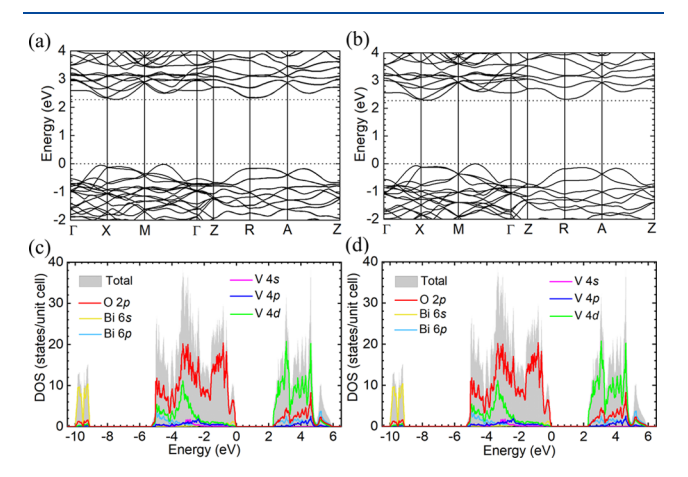


Figure 5. Calculated electronic band structure and density of states of (a, c) monoclinic and (b, d) tetragonal phases of BiVO<sub>4</sub>. The zero in the energy axis was set to the valence-band maximum in both cases.

their electronic structure. As pointed out above, the lowestenergy conduction-band states are the antibonding combination of V 3d and O 2p orbitals. Adding electrons to these conduction-band states leads to an elongation of some of the V-O bonds, which, in turn, also results in an elongation of a pair of Bi-O bonds, lowering the symmetry and driving the transformation to the monoclinic crystal structure of BiVO<sub>4</sub>. Despite the significant differences in lattice parameters and local structure between t-BiVO<sub>4</sub> and m-BiVO<sub>4</sub>, their band structures look rather similar. For both structures, the top of the valence band occurs along the line between M and  $\Gamma$ , whereas the bottom of the conduction band occurs in the line between X and M. Using the SCAN functional, the calculated indirect band gaps are 2.29 eV for t-BiVO<sub>4</sub> and 2.28 eV for m-BiVO<sub>4</sub>, while the lowest direct band gaps are 2.40 and 2.39 eV, respectively.

Energetics of m-BiVO<sub>4</sub> vs. t-BiVO<sub>4</sub> upon Doping. We calculated the total energy difference between t-BiVO<sub>4</sub> and m-BiVO<sub>4</sub> for the undoped and doped (0.25 electrons per formula unit) cases, [i.e.,  $\Delta E(n) = E_{tot}[t-BiVO_4(n)] - E_{tot}(m-1)$ BiVO<sub>4</sub>(n)], where n = 0 and 0.25. To simulate undoped m-BiVO<sub>4</sub>, we took the doped structure (n = 0.25), removed the excess electrons, and calculated the total energy without letting the system to relax. To simulate the doped t-BiVO<sub>4</sub>, we added 0.25 electron per formula unit to the optimized undoped t-BiVO<sub>4</sub>, also without letting the system to relax. As a result, we obtained  $\Delta E(0) = -0.81$  meV per formula unit and  $\Delta E(0.25)$ = 60 meV per formula unit, confirming that t-BiVO<sub>4</sub> becomes unstable with respect to m-BiVO<sub>4</sub> upon doping. The magnitude and similarity of the absolute value of these energy differences also indicate a certain symmetry in the stability of tand m-BiVO<sub>4</sub> phases with respect to doping.

#### DISCUSSION

Considering the similarities of their electronic band structures in Figure 5, it is rather unclear why m-BiVO<sub>4</sub> would show higher efficiency than m-BiVO<sub>4</sub> in the photoelectrochemical activity. A recent report suggests that the observed difference in efficiency could arise from the different grain sizes of the t and m-BiVO<sub>4</sub> samples used during experiments.<sup>38</sup> Here, we speculate that the difference in the photoelectrochemical activity might be related to surface or interface states. Since m- $BiVO_4$  is a layered structure, we expect that the (001) plane be a natural cleavage plane, where surface states do not play an important role in carrier recombination. On the other hand, in the tridimensional crystal structure of m-BiVO<sub>4</sub>, such a cleavage plane would involve surface states that would enhance carrier recombination, leading to decreased efficiency in the photoelectrochemical activity. In this case, the effect of excess electrons would be to stabilize the (layered) monoclinic crystal structure of BiVO<sub>4</sub> with its favorable surface electronic structure. We note that this is only speculative at this point, and that detailed calculations for the surface electronic structure are in progress and will be subject of a separate

We should note that small polarons were predicted to form in BiVO<sub>4</sub><sup>39</sup> through the localization of an excess electron on individual V atoms, changing its oxidation state from +5 to +4. Such phenomena were also predicted to occur in titanates, such as TiO<sub>2</sub><sup>40</sup> and SrTiO<sub>3</sub>, 41 still free electrons that contribute to conductivity with mobilities that are much higher than that given by hopping of small polarons are also observed in these materials. 42,43 Therefore, we suppose that free excess electrons could, in principle, co-exist with small polarons, and that these free electrons would induce the transformation from t- to m-BiVO<sub>4</sub>, as described above. Or it could happen that the presence of small polarons would also lead to such transformation. Studies on the impact of small polarons on the stability of t- vs m-BiVO<sub>4</sub>, however, are underway and are beyond the scope of this study in part due to the high computational cost involved.

Regarding the nature of the dopants, from a series of possible impurities, it has been found that m-BiVO<sub>4</sub> shows high PEC efficiency particularly for samples doped with the shallow donors Mo<sup>6+</sup> and W<sup>6+</sup>. It has also been argued that the incorporation of interstitial hydrogen or oxygen vacancies also leads to high PEC efficiencies. Although the reported Mo and W concentrations reported to give enhanced photocurrent were about 3-5%, i.e., less than the

electron concentration required for full transformation of tinto m-BiVO $_4$ , as discussed above, the concentrations of interstitial H or oxygen vacancies that give high PEC efficiencies are difficult to determine. It is likely that the presence of the impurities themselves, i.e., not only the excess electrons, also helps break the symmetry, perhaps lowering the required excess electron concentration. The effects of specific impurities on the phase transformation of BiVO $_4$  are also a subject of future study.

# CONCLUSIONS

We show that excess electrons play an important role in determining the phase of BiVO<sub>4</sub>. The electrochemically active monoclinic m-BiVO<sub>4</sub> is unstable when undoped, spontaneously transforming to the tetragonal phase t-BiVO<sub>4</sub>. Adding electrons to the conduction band of t-BiVO4, we see it transforming to m-BiVO<sub>4</sub>, where pairs of V-O bonds and Bi-O bonds become elongated, thus lowering the symmetry of the VO<sub>4</sub> and BiO<sub>8</sub> polyhedra. Despite the differences in lattice parameters and the local structure of the VO<sub>4</sub> and BiO<sub>8</sub> polyhedra, we find that t-BiVO<sub>4</sub> and m-BiVO<sub>4</sub> have rather similar band structures, leading us to speculate that the differences between the electrochemical activity of these two phases must be related to carrier recombination at surfaces or interfaces. The layered structure of m-BiVO<sub>4</sub> would lead to rather ineffective recombination channels at the surface of natural cleavage, as opposed to the tridimensional structure of t-BiVO<sub>4</sub>, whose surface states would lead to higher carrier recombination, hindering its photoelectrochemical activity. Doping would then be crucial for stabilizing m-BiVO<sub>4</sub>, which is the one related to the higher photoelectrochemical activity.

# AUTHOR INFORMATION

## **Corresponding Author**

\*E-mail: laraib@udel.edu, janotti@udel.edu

#### ORCID

Iflah Laraib: 0000-0003-0731-1795

#### **Notes**

The authors declare no competing financial interest.

# ACKNOWLEDGMENTS

This work was funded by the NSF Early Career Award grant No. DMR-1652994. It made use of the computing resources provided by the Extreme Science and Engineering Discovery Environment (XSEDE), supported by the National Science Foundation grant number ACI-1053575 and the Information Technologies (IT) resources at the University of Delaware, specifically the high-performance computing resources.

### REFERENCES

- (1) Bockris, J. The origin of ideas on a hydrogen economy and its solution to the decay of the environment. *Int. J. Hydrogen Energy* **2002**, *27*, 731–740.
- (2) Barreto, L.; Makihira, A.; Riahi, K. The hydrogen economy in the 21st century: A sustainable development scenario. *Int. J. Hydrogen Energy* **2003**, 28, 267–284.
- (3) Fujishima, A.; Honda, K. Electrochemical photolysis of water at a semiconductor electrode. *Nature* **1972**, 238, 37–38.
- (4) Khaselev, O. A monolithic photovoltaic-optoelectrochemical device for hydrogen production via water splitting. *Science* **1998**, *280*, 425–427.

- (5) Walter, M. G.; Warren, E. L.; McKone, J. R.; Boettcher, S. W.; Mi, Q.; Santori, E. A.; Lewis, N. S. Solar water splitting cells. *Chem. Rev.* **2010**, *110*, 6446–6473.
- (6) Chen, X.; Shen, S.; Guo, L.; Mao, S. S. Semiconductor-based photocatalytic hydrogen generation. *Chem. Rev.* **2010**, *110*, 6503–6570.
- (7) Sivula, K.; van de Krol, R. Semiconducting materials for photoelectrochemical energy conversion. *Nat. Rev. Mater.* **2016**, *1*, No. 16010.
- (8) Abdi, F. F.; Han, L.; Smets, A. H. M.; Zeman, M.; Dam, B.; Krol, R. V. D. Efficient solar water splitting by enhanced charge separation in a bismuth vanadate-silicon tandem photoelectrode. *Nat. Commun.* **2013**. *4*. No. 2195.
- (9) Jiang, C.; Moniz, S. J.; Wang, A.; Zhang, T.; Tang, J. Photoelectrochemical devices for solar water splitting-materials and challenges. *Chem. Soc. Rev.* **2017**, *46*, 4645–4660.
- (10) Zhao, Z.; Li, Z.; Zou, Z. Electronic structure and optical properties of monoclinic clinobisvanite BiVO<sub>4</sub>. *Phys. Chem. Chem. Phys.* **2011**, 4746–4753.
- (11) Cooper, J. K.; Gul, S.; Toma, F. M.; Chen, L.; Glans, P. A.; Guo, J.; Ager, J. W.; Yano, J.; Sharp, I. D. Electronic structure of monoclinic BiVO<sub>4</sub>. *Chem. Mater.* **2014**, *26*, 5365–5373.
- (12) Cooper, J. K.; Gul, S.; Toma, F. M.; Chen, L.; Liu, Y. S.; Guo, J.; Ager, J. W.; Yano, J.; Sharp, I. D. Indirect bandgap and optical properties of monoclinic bismuth vanadate. *J. Phys. Chem. C* **2015**, 119, 2969–2974.
- (13) Park, Y.; McDonald, K. J.; Choi, K.-S. Progress in bismuth vanadate photoanodes for use in solar water oxidation. *Chem. Soc. Rev.* **2013**, *42*, 2321–2337.
- (14) Kim, T. W.; Ping, Y.; Galli, G. A.; Choi, K. S. Simultaneous enhancements in photon absorption and charge transport of bismuth vanadate photoanodes for solar water splitting. *Nat. Commun.* **2015**, *6*, No. 8769.
- (15) Frost, R. L.; Henry, D. A.; Weier, M. L.; Martens, W. Raman spectroscopy of three polymorphs of BiVO <sub>4</sub>: Clinobisvanite, dreyerite and pucherite, with comparisons to V<sub>4</sub>O<sub>3</sub>-bearing minerals: namibite, pottsite and schumacherite. *J. Raman Spectrosc.* **2006**, *37*, 722–732.
- (16) Qurashi, M. M.; Barnes, W. H. A preliminary structure for pucherite, BiVO<sub>4</sub>. Am. Mineral. 1952, 37, 423–426.
- (17) Roth, R. S.; Waring, J. L. Synthesis and stability of bismutotantalite, stibiotantalite, and chemically similar ABO<sub>4</sub> compounds. *Am. Mineral.* **1963**, 48, 1348–1356.
- (18) Ding, K.; Chen, B.; Fang, Z.; Zhang, Y. Density functional theory study on the electronic and optical properties of three crystalline phases of BiVO<sub>4</sub>. *Theor. Chem. Acc.* **2013**, *132*, No. 1352.
- (19) Tokunaga, S.; Kato, H.; Kudo, A. Selective preparation of monoclinic and tetragonal BiVO<sub>4</sub> with scheelite structure and their photocatalytic properties. *Chem. Mater.* **2001**, *13*, 4624–4628.
- (20) Bhattacharya, A. K.; Mallick, K. K.; Hartridge, A. Phase transition in BiVO<sub>4</sub>. Mater. Lett. 1997, 30, 7–13.
- (21) Sleight, A. W.; Chen, H. Y.; Ferretti, A.; Cox, D. E. Crystalgrowth and structure of BiVO<sub>4</sub>. *Mater. Res. Bull.* **1979**, *14*, 1571–1581.
- (22) David, W. I. F. Ferroelastic phase transition in BiVO 4: IV. Relationships between spontaneous strain and acoustic properties. *J. Phys. C: Solid State Phys.* 1983, 16, 5119–5126.
- (23) David, W. I. F.; Glazer, A. M.; Hewat, A. W. The structure and ferroelastic phase transition of BiVO<sub>4</sub>. *Phase Transitions* **1979**, 1, 155–169
- (24) Park, H. S.; Kweon, K. E.; Ye, H.; Paek, E.; Hwang, G. S.; Bard, A. J. Factors in the metal doping of BiVO<sub>4</sub> for improved photoelectrocatalytic activity as studied by scanning electrochemical microscopy and first-principles density-functional calculation. *J. Phys. Chem. C* 2011, 115, 17870–17879.
- (25) Yin, W. J.; Wei, S. H.; Al-Jassim, M. M.; Turner, J.; Yan, Y. Doping properties of monoclinic BiVO<sub>4</sub> studied by first-principles density-functional theory. *Phys. Rev. B* **2011**, *83*, No. 155102.

- (26) Kweon, K. E.; Hwang, G. S. Hybrid density functional study of the structural, bonding, and electronic properties of bismuth vanadate. *Phys. Rev. B* **2012**, *86*, No. 165209.
- (27) Wang, G.; Ling, Y.; Lu, X.; Qian, F.; Tong, Y.; Zhang, J. Z.; Lordi, V.; Rocha Leao, C.; Li, Y. Computational and photoelectrochemical study of hydrogenated bismuth vanadate. *J. Phys. Chem. C* 2013, 117, 10957–10964.
- (28) Kohn, W.; Sham, L. J. Self-consistent equations including exchange and correlation effects. *Phys. Rev.* **1965**, *140*, A1133–A1138.
- (29) Hohenberg, P.; K, W. Inhomogeneous electron gas. *Phys. Rev.* **1964**, *136*, B864–B871.
- (30) Kresse, G.; Hafner, J. Ab initio molecular dynamics for liquid metals. *Phys. Rev. B* **1993**, *47*, 558–561.
- (31) Kresse, G.; Hafner, J. Ab initio molecular-dynamics simulation of the liquid-metal-amorphous-semiconductor transition in germanium. *Phys. Rev. B* **1994**, *49*, 14251–14269.
- (32) Blöchl, P. E. Projector augmented-wave method. *Phys. Rev. B* **1994**, *50*, 17953–17979.
- (33) Perdew, J. P.; Burke, K.; Ernzerhof, M. Generalized gradient approximation made simple. *Phys. Rev. Lett.* **1996**, *77*, 3865–3868.
- (34) Csonka, G. I.; Perdew, J. P.; Ruzsinszky, A.; Philipsen, P. H. T.; Lebègue, S.; Paier, J.; Vydrov, O. A.; Ángyán, J. G. Assessing the performance of recent density functionals for bulk solids. *Phys. Rev. B* **2009**, *79*, No. 155107.
- (35) Sun, J.; Remsing, R. C.; Zhang, Y.; Sun, Z.; Ruzsinszky, A.; Peng, H.; Yang, Z.; Paul, A.; Waghmare, U.; Wu, X.; et al. Accurate first-principles structures and energies of diversely bonded systems from an efficient density functional. *Nat. Chem.* **2016**, *8*, 831–836.
- (36) Heyd, J.; Scuseria, G. E.; Ernzerhof, M. Hybrid functionals based on a screened Coulomb potential. *J. Chem. Phys.* **2003**, *118*, 8207–8215.
- (37) Wiktor, J.; Reshetnyak, I.; Ambrosio, F.; Pasquarello, A. Comprehensive modeling of the band gap and absorption spectrum of BiVO<sub>4</sub>. *Phys. Rev. Mater.* **2017**, *1*, No. 022401.
- (38) Newhouse, P. F.; Guevarra, D.; Umehara, M.; Reyes-Lillo, S. E.; Zhou, L.; Boyd, D. A.; Suram, S. K.; Cooper, J. K.; Haber, J. A.; Neaton, J. B.; et al. Combinatorial alloying improves bismuth vanadate photoanodes via reduced monoclinic distortion. *Energy Environ. Sci.* **2018**, *11*, 2444–2457.
- (39) Kweon, K. E.; Hwang, G. S.; Kim, J.; Kim, S.; Kim, S. Electron small polarons and their transport in bismuth vanadate: a first principles study. *Phys. Chem. Chem. Phys.* **2015**, *17*, 256–260.
- (40) Selcuk, S.; Selloni, A. Facet-dependent trapping and dynamics of excess electrons at anatase TiO<sub>2</sub> surfaces and aqueous interfaces. *Nat. Mater.* **2016**, *15*, 1107–1112.
- (41) Frederikse, H. P. R.; Thurber, W. R.; Hosler, W. R. Electronic transport in strontium titanate. *Phys. Rev.* **1964**, *134*, A442–A445.
- (42) Forro, L.; Chauvet, O.; Emin, D.; Zuppiroli, L.; Berger, H.; Lévy, F. High mobility n-type charge carriers in large single crystals of anatase (TiO<sub>2</sub>). *J. Appl. Phys.* **1994**, *75*, 633–635.
- (43) Tufte, O. N.; Chapman, P. W. Electron mobility in semiconducting strontium titanate. *Phys. Rev.* **1967**, *155*, 796–802.
- (44) Luo, W.; Yang, Z.; Li, Z.; Zhang, J.; Liu, J.; Zhao, Z.; Wang, Z.; Yan, S.; Yu, T.; Zou, Z. Solar hydrogen generation from seawater with a modified BiVO<sub>4</sub> photoanode. *Energy Environ. Sci.* **2011**, *4*, 4046–4051
- (45) Zhong, D. K.; Choi, S.; Gamelin, D. R. Near-complete suppression of surface recombination in solar photoelectrolysis by "Co-Pi" catalyst-modified W:BiVO<sub>4</sub>. *J. Am. Chem. Soc.* **2011**, *133*, 18370–18377.